Journal of Chromatography, 469 (1989) 53–65
Elsevier Science Publishers B.V., Amsterdam — Printed in The Netherlands

CHROM. 21 335

CONTRIBUTION OF LONGITUDINAL DIFFUSION TO BAND BROADENING IN LIQUID CHROMATOGRAPHY

ALAIN BERTHOD*, FRÉDÉRIC CHARTIER and JEAN-LOUIS ROCCA
Laboratoire des Sciences Analytiques, UA CNRS 435, Université de Lyon 1, 69622 Villeurbanne Cédex (France)

(First received December 27th, 1988; revised manuscript received January 20th, 1989)

SUMMARY

The contribution of longitudinal diffusion to band broadening in liquid chromatography was studied with a laboratory-made densely grafted stationary phase. Nucleosil 100-5 was used as the silica base. Tetradecyldimethyl(dimethylamino)silane was the bonding reagent used to obtain a brush-type monolayer phase with an 18% carbon load and 3.5 μmol/m^2 bonding coverage. The phase was fully characterized for surface area, porosity and mean pore diameter. A 15 cm × 4 mm I.D. column was slurry packed with the phase and used to obtain Knox plots: h, the reduced plate height, *versus* v, the reduced linear mobile phase velocity. All efficiency values were measured using the moment method. A, B and C terms of the Knox equation were determined at two temperatures, 25 and 40°C, and for four solutes, benzene, toluene, ethylbenzene and propylbenzene. As longitudinal diffusion is dependent on B, B values were also determined by the arrested elution method (static method). Static and dynamic plots of B *versus* k' led to obstruction factors, γ_m, of 1.10 ± 0.1 and 1.32 ± 0.16, respectively. If obstruction factors higher than unity are found with other phases, it may be thought that the established chromatographic theory overlooked some phenomena occurring in porous and densely bonded phases.

INTRODUCTION

One of the constant trends in liquid chromatography (LC) is attempts to achieve more efficient systems. The understanding of the causes of band broadening is the obvious way to control and to reduce it. The earliest mathematical description of the general phenomena occurring in a chromatographic column was developed by Martin and Synge[1], who introduced the plate model still in use today. This model was refined by several workers, specially Giddings[2] and Knox and co-workers[3–7]. Several models, such as the mass balance model, were developed. The random walk model and the non-equilibrium treatment were both initiated by Giddings[2]. Using these models, different plate-height equations were derived by Giddings[2], Snyder[8], Huber[9] and Knox and co-workers[3,4]. Such equations relate the reduced plate height to the reduced mobile phase velocity. With a set of experiments at different flow-rates, it is possible to obtain an insight into the solute exchange between phases in the column.

0021-9673/89/$03.50

The aim of this work was to study the contribution of the longitudinal diffusion to band broadening. The B term of the Knox equation is directly related to the longitudinal or axial molecular diffusion. The Knox equation is

$$h = Av^{1/3} + B/v + Cv \tag{1}$$

in which A, B and C are dimensionless solute and stationary zone-dependent constants, h is the dimensionless reduced plate height [$h = H/d_p$, where H is the height equivalent to a theoretical plate (HETP) and d_p is the particle diameter] and v is the dimensionless reduced velocity:

$$v = ud_p/D_m \tag{2}$$

where u is the mobile phase linear velocity (cm/s), and D_m the solute diffusion coefficient in the mobile phase (cm^2/s). It is relatively easy to obtain the A, B and C terms of the Knox equation by measuring efficiencies at different mobile phase flow-rates.

In most studies, the chromatographic peak efficiencies were derived from peak-width measurements assuming a Gaussian peak shape. Such calculations always produce overestimated plate numbers. Throughout this work, the moment method was used for efficiency measurement, as it is the only method that makes no assumptions about the peak shape[2].

Such efficiency experiments were usually done with commercial stationary phases for which the physico-chemical properties are not fully known. In order to work on a well characterized phase, we synthesized it and packed a column with it. To cross-check the results obtained dynamically (Knox equation), static experiments (non-elution chromatography) were carried out with the same column.

THEORETICAL

The HETP is the ratio of the column length, L, to the plate number, N:

$$H = L/N \tag{3}$$

Expressing the peak variance, σ^2, in length units, the HETP becomes

$$H = \sigma^2/L \tag{4}$$

Variances are additive. The total variance, σ^2, is the sum of several contributions:

$$\sigma^2 = \sigma^2_{ext} + \sigma^2_{fl} + \sigma^2_{ld} + \sigma^2_{mt} \tag{5}$$

where the subscripts ext, fl, ld and mt represent the extra-column contributions (injector, detector, tubing), the flow contribution (eddy diffusion and flow anisotropy), the longitudinal diffusion contribution (the term investigated in this study) and the mass transfer term, respectively.

For a column packed with porous particles, the general plate height expression was written as[2]

$$H = 2\lambda d_p + 2\gamma D_m/u + \frac{qk'd_f^2u}{(1 + k')^2D_s} + \frac{[\Omega f(k') + f(\varphi)g(k')]\, ud_p^2}{D_m} \tag{6}$$

where λ, γ, q and Ω are geometrical factors, D_m and D_s are the diffusion coefficients of the solute in the mobile and the stationary phase, respectively, k' is the capacity factor, d_f is the stationary phase thickness, φ is the fraction of the mobile phase inside the porous bed and $f(k')$, $g(k')$ and $f(\varphi)$ are mathematical functions.

Knox[6] showed that the flow contribution to the plate height equation could be represented to a high degree of approximation by

$$H_{fl} = [1/(\alpha + \beta u^{-n})] \qquad \text{with } n < 1 \tag{7}$$

where α and β are constants and n, determined empirically, has a value between 0.2 and 0.5. Using the reduced parameters h and v, Knox further simplified eqn. 7 to

$$h_{fl} = Av^{1/3} \tag{8}$$

The constant A depends critically on the regularity of the column packing, A very uniform column packing may produce an A value as low as 0.5. Values of A larger than 3 usually indicate a poorly packed column[6].

The C term of the Knox equation (eqn. 1) represents the mass transfer contribution. According to Giddings[2], Knox[6] and Knox and Scott[10], it can be written as

$$C = q\left(\frac{k' + \varphi}{1 + k'}\right)^2\left(\frac{D_m}{\gamma_{sm}\varphi D_m + k'\gamma_s D_s}\right) \tag{9}$$

where the subscript sm represents the stagnant mobile phase and the γ terms are obstruction factors for diffusion through granular and/or porous materials. The geometrical factor q is dependent on porosity[2]. For a stationary phase in a spherical configuration and medium pores, $q = 1/30$. For narrow pores whose cross-sectional area, a, increases from the bottom as $a = a_0x^n$, where x is the distance from the bottom of the pore and n is the taper factor, q becomes $2/[(n + 1)(n + 3)]$. For example, when the taper factor is 2, $q = 2/15$.

The B term of the Knox equation is the term of interest in longitudinal diffusion studies. Using the random walk model and the Einstein equation for molecular diffusion[11], which is

$$d^2 = 2\, Dt_d \tag{10}$$

where t_d is the average time which a molecule needs to diffuse a distance d from its starting point, Giddings[2] showed that the longitudinal molecular diffusion contribution is the sum of three terms:

a stationary phase term:

$$\sigma_s^2 = 2\gamma_s D_s k' V_m \tag{11}$$

a moving mobile phase term (subscript mm):

$$\sigma_{mm}^2 = 2\gamma_{mm} D_m (1 - \varphi) V_m \tag{12}$$

and a stagnant mobile phase term:

$$\sigma_{sm}^2 = 2\gamma_{sm} D_m \varphi V_m \tag{13}$$

Using the reduced parameters h and v and restricting the sum $[\gamma_{mm}(1 - \varphi) + \gamma_{sm}\varphi]$ to γ_m, the B term can be written as

$$B = 2 [\gamma_m + \gamma_s (D_s/D_m) k'] \tag{14}$$

SYNTHESIS AND CHARACTERIZATION OF THE STATIONARY PHASE

The stationary phase was synthesized following the aminosilane route described by Kováts and co-workers[12,13]. Aminosilanes are known to produce highly dense and reproducible organosiloxy brush-type layers[12].

It was shown by Morel and co-workers[14,15] that thermal phase transitions occurred for densely grafted alkyl phases. The transition temperature was closely related to the melting point of the corresponding linear alkane. For example, the transition zone of brush-type octadecylsilane (ODS, C_{18}) phases was between 7 and 27°C and the melting point of *n*-octadecane is 28°C. This phase transition for ODS-bonded silica corresponds to the most usual working temperatures and may be responsible for the lack of reproducibility obtained using such phases. We chose to prepare a tetradecyl (C_{14}) bonded phase because the melting point of tetradecane is 5°C and, hopefully, the thermal transition zone will be well below room temperature.

Synthesis

A thorough description of the stationary phase synthesis and characterization was given in a recent paper[16]. Nucleosil 100-5 silica base was obtained from Macherey, Nagel & Co. (Düren, F.R.G.). This spherical silica was stated to have a mean particle size, mean pore diameter and pore volume of 5 μm, 10 nm and 1 ml/g, respectively. The actual values for the batch used were measured and are given in Table I. The pore volume and diameter were 38% and 27%, respectively, lower than the supplier's stated values. The bonding reagent was tetradecyl(dimethylamino)silane prepared from tetradecene[16].

Characterization

Table I lists the physico-chemical parameters of the bare Nucleosil 100-5 compared with these of the bonded material. Surface areas were measured using the BET method. Pore size and pore volume were obtained by the mercury intrusion method. A Carlo Erba mercury porosimeter was used. Carbon loading percentages

TABLE I

STATIONARY PHASE PARAMETERS

Stationary phase	*Surface area* (m^2/g)	*Particle diameter* (μm)	*Pore volume* (ml/g)	*Mean pore diameter* (nm)	*Carbon load* (%)	*Bonding coverage* ($\mu mol/m^2$)
Nucleosil 100-5	350	5	0.63	7.3	–	–
C_{14} bonded phase	210	5	0.45	8.6	17.9	3.5

and bonding coverage were calculated using C and H microanalysis measurements performed by the Service Central d'Analyses, CNRS (Solaize, France).

Nucleosil 100-5 silica gel is a highly porous material. More than 98% of the surface area is due to pores, *i.e.*, the total surface area is mainly particle internal area. The bonding procedure decreased both the surface area and pore volume. However, it seemed to increase the mean pore diameter. This value was calculated using the surface area, S, the pore volume, V_{pore}, and assuming cylindrical pores of constant diameter, d_{pore}:

$$d_{pore} = 4V_{pore}/S \tag{15}$$

The mercury intrusion curves indicated a high pore dispersity. Hence the mean pore diameter given by eqn. 15 is only indicative. However, the increase in d_{pore} after bonding was a good indication of possible clogging of filling of smaller pores due to the bonding process.

The high carbon load (17.9% for C_{14}) corresponded to a high bonding coverage (3.5 $\mu mol/m^2$) of the monolayer brush type. This bonding coverage corresponded to 78% of the theoretical maximum monolayer concentration (4.5 $\mu mol/m^2$) (ref. 17).

EXPERIMENTAL

Chromatograph system

All measurements were carried out using a standard high-performance liquid chromatography system with methanol–water (70:30, v/v) as the mobile phase at 25 or 40°C. The pump was a Shimadzu Model LC-5A (Touzart & Matignon, Paris, France). A Model 7520 0.5-μl injection valve (Rheodyne, Cotati, CA, U.S.A.) and a Shimadzu SPD-6A UV detector with a 0.5-μl cell were connected with a 15 cm × 4 mm I.D. column slurry packed with the C_{14} bonded silica described previously. The column was immersed in a constant-temperature water-bath at 25 or 40 ± 0.1°C. The solutes, benzene, toluene, ethylbenzene and propylbenzene, supplied by Merck (Darmstadt, F.R.G.), were detected at 254 nm.

Column parameters

Table II lists the column parameters. The mobile phase volume, V_m, was obtained through the density method[10]. The column was filled first with chloroform, weighed, rinsed and then filled with hexane and weighed again. The difference in weights divided by the difference in liquid densities gave V_m. The extra-particle

TABLE II

COLUMN PARAMETERS

Parameter	*Value*	*Parameter*	*Value*
Column length, L	15 cm	Stagnant mob. phase fraction,	
Column I.D.	4 mm	$\varphi = (V_m - V_{ext})/V_m$	0.37
Column volume, V_c	1885 µl	Total column porosity,	
Stationary phase volume, V_s	509 µl	$\varepsilon_T = V_m/V_c$	0.73
Mobile phase volume, V_m	1376 µl	Extra particle porosity,	
Extra particle volume, V_{ext}	868 µl	$\varepsilon_e = V_{em}/V_c$	0.46
Pore volume, V_{int}	508 µl	Column permeability factor, Φ	1500

volume, V_{em}, was obtained using sulphanilic acid. This solute is fully excluded with methanol and sodium nitrate (10^{-3} mol/l) as the mobile phase[10].

Efficiency measurements

To be able to obtain a meaningful Knox plot, the plate count must be significant. The moment method is the only method that gives the plate number of a peak with no shape assumptions[18]. Peak area is the zeroth moment, μ_0, calculated as

$$\mu_0 = \int C(t)\,\mathrm{d}t \tag{16}$$

where $C(t)$ is the detector signal. The mean is the first moment, μ_1, of the elution curve and it occurs at the centre of mass of the peak:

$$\mu_1 = \left[\int tC(t)\,\mathrm{d}t\right] \Big/ \mu_0 \tag{17}$$

The second central reduced moment, μ'_2, is the peak variance. The third moment measures the peak skewness and is not needed for plate count determination. The plate number is determined as

$$N = \mu_1^2/\mu'_2 \tag{18}$$

Moments were calculated using a Hewlett-Packard HP-85 microcomputer and a data acquisition technique. The analogue detector output was digitized by a 760 A–D interface (Nelson Analytical, Santa Clara, CA, U.S.A.). The computation method has been described elsewhere[19].

Diffusion coefficient measurements

The Taylor–Aris method[20] was used for diffusion coefficient determinations. In an open straight tube of length L and radius r, the band broadening due to the flow-rate, F, produces a variance, σ^2, dependent on the solute diffusion coefficient, D_m, according to[21]

$$\sigma^2 = \pi r^4 LF/(24D_m) \tag{19}$$

We used a water-jacketed straight tube of 1.60 m × 0.254 mm (1/100 in.) I.D. and an internal volume of 83 μl. Total variances were determined for five different flow-rates, 10, 20, 50, 100 and 200 μl/min. They were corrected for the extra-column band broadening (Fig. 1). D_m was obtained from the slopes of the σ^2 *versus* F plots.

Arrested elution method

All B values were checked by the arrested elution method[22]. Band broadening arising from longitudinal diffusion is independent of whether the band is moving or stationary. If the solute is stopped inside the column for a time t_r, axial diffusion occurs and induces an additional variance, σ_z^2, which increases the total variance:

$$\sigma_z^2 = 2D_{eff}t_r \tag{20}$$

where D_{eff} is the effective diffusion coefficient of the solute in the column. t_r was varied from 2 to 15 h. The plots of the total variance, σ^2, *versus* t_r gave straight lines whose slopes led to D_{eff}[10,22]. D_{eff} is related to γ_m, k' and γ_s by[10]

$$D_{eff} = (\gamma_m D_m + k'\gamma_s D_s)/(1 + k') \tag{21}$$

Eqns. 14 and 21 give:

$$B = 2(1 + k')\, D_{eff}/D_m \tag{22}$$

Extra-column band broadening

Eqn. 5 shows an extra-column contribution, σ_{ext}^2, to the total measured variance, σ^2. This contribution was calculated by measuring the variance obtained with the injection valve directly connected to the UV detector, without a column or straight tube. Fig. 1 shows the external variance *versus* flow-rate. All measured variances were corrected for the corresponding σ_{ext}^2 value.

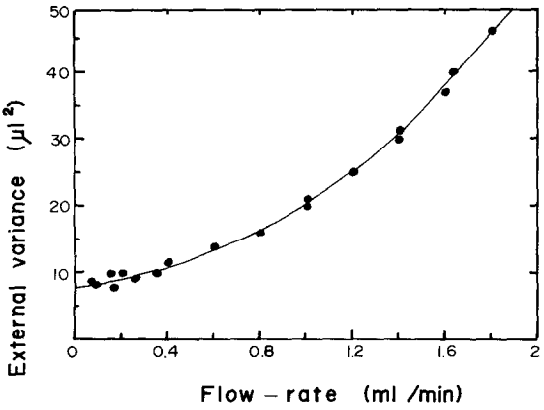

Fig. 1. Dependence of the external variance on the flow-rate. Mobile phase, methanol–water (70:30, v/v); test solute, benzene; variances measured with the moment method.

RESULTS AND DISCUSSION

Diffusion coefficient measurements

Table III lists the diffusion coefficients, D_m and D_{eff}, for the four solutes studied at 25 and 40°C. All D_m values at 40°C were obtained by correcting the corresponding 25°C D_m value for temperature, T, and viscosity, η, changes:

$$D_{m40} = D_{m25}\ (313/298)\ (\eta_{25}/\eta_{40}) = 1.355\ D_{m25} \tag{23}$$

A, B and C terms of the Knox equation

Table IV gives the efficiency obtained at different flow-rates. Plate numbers, N, as high as 7000 were obtained for a 15-cm column, corresponding to about 50 000 plate/m [70 000 plate/m assuming a Gaussian shape for the peaks (0.6H method)]; 0.6H N values are given for information but were not used in this work. The moment values of N are generally smaller than the 0.6H values by a factor of 40%. The 0.6H values were corrected for extra-column effects using the external variances (Fig. 1) obtained with the moment method. The corresponding external variances calculated by the 0.6H method would be lower. Then the corrected 0.6H plate values would also be lower. This would bring the two values more closely into line. As the experimental system was optimized to reduce all external contribution (Fig. 1), the typical N discrepancy would stay in the region of 30%.

Table V lists the computer-fitted values (least-squares method) of the A, B and C terms of the Knox equation together with the capacity factors, k', at 25 and 40°C. The A term, close to unity, is an indication of a correctly packed column[3–7]. For the four solutes studied, A seems not to be dependent on k' and slightly dependent on temperature. The mean values were 1.1 and 0.9 at 25 and 40°C, respectively.

The C term measures the efficiency of the mass transfer. The column and stationary phase particles that we used were not well suited for a reliable C determination. The maximum reduced velocity value that we were able to obtain was lower than 20 in order to work with a reasonable column pressure drop. Knox and Pryde[23] recommend the use of v values higher than 100 in order to obtain a significant C evaluation. Knox and Scott[10] used v values as high as 5000 with 540-μm particles. This was impossible with 5-μm particles and 15-cm columns as the inlet pressure very rapidly became the limiting factor. At 25°C, the C values decreased as k' increased (Table V). An identical trend was reported by Stout *et al.*[24]. They thought that the

TABLE III

SOLUTE DIFFUSION COEFFICIENTS ($\times$ 10^6 cm^2/s)

Coefficient	*Temperature (°C)*	*Solute*			
		Benzene	*Toluene*	*Ethylbenzene*	*Propylbenzene*
D_m	25	8.65	8.0	7.4	6.5
	40	11.8	10.8	10.0	8.8
D_{eff}	25	5.6	4.45	3.3	2.5
	40	7.9	6.7	5.0	4.2

TABLE IV

EFFICIENCY MEASUREMENTS AT 25°C

Plate count obtained by the moment method or by $N = 4(t_r/W_{0.6H})^2$ for the $N(0.6H)$ columns. Average of at least three coherent (within 5%) experiments.

Flow-rate (ml/min)	*Benzene*		*Toluene, N*	*Ethylbenzene, N*	*Propylbenzene*	
	N	*N(0.6H)*			*N*	*N(0.6H)*
0.078	5860	6070	5670	–	–	–
0.088	6060	5920	6030	5240	4610	4870
0.099	7335	7360	6145	5860	5190	5375
0.196	9110	11 010	9160	6720	5585	5940
0.291	9260	11 475	9880	8860	8490	8810
0.389	8260	10 800	9160	9070	8810	9890
0.489	8630	10 190	9055	8400	8210	10 150
0.569	7620	11 680	8250	8110	8200	9770
0.688	6695	11 030	7780	6880	7430	9620
0.791	6330	9980	7310	6980	7550	10 460
0.891	6070	10 600	7045	6730	6780	9770
0.985	6570	10 800	7305	5930	6590	10 190
1.080	6120	11 610	6665	5890	6650	10 035
1.160	6110	11 550	6485	5290	6200	10 225
1.230	6285	11 920	5860	5090	6050	9850

decrease in C with increasing k' was due to surface diffusion as the effective diffusion coefficient of solute molecules would be greater within the particle pores as a result of surface diffusion. Horváth and Lin[25] also demonstrated that the plate height contribution of kinetic resistances was dependent on k'. The decrease in C with increase in k' was less obvious at 40°C. The general trend is an increase in C with increase in temperature. This may be due to the temperature dependence of diffusion coefficients, as shown by eqn. 9 and Table III.

TABLE V

KNOX PARAMETERS AND CAPACITY FACTORS

Error limits in parentheses. Range of v, 0.7–16; number of data points, 15 (see Table IV).

Solute	*25°C*					*40°C*				
	A	*B*	*B*[a]	*C*	*k'*	*A*	*B*	*B*[a]	*C*	*k'*
Benzene	1.1 (0.15)	3.1 (0.2)	2.72 (0.03)	0.22 (0.02)	1.1	1.1 (0.25)	4.5 (0.7)	2.54 (0.03)	0.2 (0.04)	0.9
Toluene	1.05 (0.15)	3.5 (0.2)	3.45 (0.03)	0.16 (0.02)	2.1	0.85 (0.25)	4 (0.7)	3.22 (0.03)	0.34 (0.04)	1.6
Ethylbenzene	1.1 (0.15)	3.8 (0.4)	4.01 (0.04)	0.15 (0.02)	3.5	0.9 (0.15)	3.5 (0.4)	3.60 (0.04)	0.32 (0.03)	2.6
Propylbenzene	1.3 (0.15)	5.0 (0.4)	5.38 (0.04)	0.09 (0.02)	6.0	0.8 (0.10)	5.0 (0.5)	5.15 (0.04)	0.21 (0.02)	4.4

[a] B values obtained by the arrested elution method (eqn. 22).

Table VI lists the characteristics of the plots of $(q/C)\,[(k' + \varphi)/(1 + k')]^2$ *versus* k'. According to eqn. 9, these plots must be linear with $\gamma_s D_s/D_m$ as the slope and $\gamma_{sm}\varphi$ as the intercept. Two q values were used to obtain these plots; $q = 1/30$ is the value usually chosen for porous spherical particles and $q = 2/15$ corresponds to a stationary phase with narrow pores and a taper factor of 2 (from ref. 2, p. 190). Given the low accuracy of C determination, the linearity was not very good (regression factors $r^2 = 0.979$ and 0.715 at 25 and 40°C, respectively). For comparison, the values in ref. 24 were plotted using the same procedure. The results in Table VI were compared with those obtained by static and dynamic experiments leading to the B term which is the term of interest in longitudinal diffusion studies. Table V gives the B terms obtained by dynamic and static experiments.

Comparison of dynamic and static results

The B values obtained by fitting the h *versus* v plots with the Knox equation were in agreement with those obtained by the arrested elution method for all sets of experiments except with benzene and toluene at 40°C. Attempts were made to fit the dynamic experimental results using the static B values. The A and C values resulting from such a fitting procedure were within the limits indicated in Table V, except for benzene and toluene at 40°C.

Plots of B *versus* k' at 25 and 40°C are shown in Fig. 2A and B, respectively. The static B values obtained from Table III and eqn. 22 correspond to open symbols and the dynamic values (Table V, eqn. 14) to closed symbols. Lines 2 and 3 match the maximum and minimum errors in Table V to give an idea of the uncertainty in γ_m. Table VII lists the slopes, intercepts, regression coefficients and calculated chromatographic parameters. The surprising result is the high value of γ_m, the mobile phase obstruction factor. At 25°C, the intercepts led to γ_m values of 1.32 ± 0.16 and 1.10 ± 0.04 for dynamic and static experiments, respectively. These results cannot be attributed to experimental errors, given the relatively low scatter of data and the same trend obtained by two different approaches. Values very close to unity were obtained for the obstruction factor γ_m[7–10]. B data from ref. 24 were calculated from peak

TABLE VI

PARAMETERS CORRESPONDING TO C VALUES

Slopes and intercepts of the $(q/C)\,[(k' + \varphi)/(1 + k')]^2$ *versus* k' plots (eqn. 9); n = number of points.

q	*Temperature* (°C)	*Slope* ($\gamma_s D_s/D_m$)	*Intercept* ($\gamma_{sm}\varphi$)	r^2	n	γ_{sm}
1/30	25	0.046	0.023	0.979	4	0.062
		0.016	0.042	0.715	4	0.113
	22	0.063[a]	0.27[a]	0.764[a]	9[a]	0.900[a]
		0.046[b]	0.05[b]	0.826[b]	16[b]	0.255[b]
2/15	25	0.184	0.092	0.979	4	0.248
		0.065	0.170	0.715	4	0.460
	22	0.252[a]	1.09[a]	0.764[a]	9[a]	3.650[a]
		0.182[b]	0.20[b]	0.826[b]	16[b]	1.020[b]

[a] 3- and 6-μm Zorbax C_8 phase.

[b] 3- and 6-μm Zorbax C_{18} phase, from Table I in ref. 24.

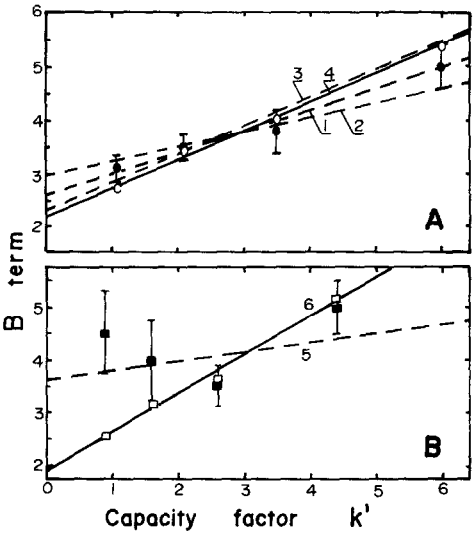

Fig. 2. Plots of *B versus k'*. Open symbols and solid lines: static determination (eqn. 22 and Table III). Closed symbols and dashed lines: dynamic determination (Knox plots, Table V). Column, 15 cm × 4 mm I.D.; C_{14} stationary phase; mobile phase, methanol–water (70:30, v/v). (A) 25°C. 1, Dynamic determination, mean; 2, dynamic determination, minimum; 3, dynamic determination, maximum; 4, static determination, see Table VII. (B) 40°C. 5, Dynamic determination; 6, static determination.

efficiencies obtained using the moment method. These data were force-fitted to a γ_m value of 0.64. Although the scatter of these data were not completely inconsistent with $\gamma_m = 0.64$, Fig. 3 in ref. 24 appears unusual. We further used them to construct *B versus k'* plots, without any force-fitted value. The slopes and intercepts of such plots are listed in Table VII. This allowed us to calculate γ_m values higher than unity for porous Zorbax commercial stationary phases, considering plots with r^2 lower than 0.95 are significant. A γ_m value higher than 1 is theoretically impossible[2]; it would mean that solute diffusion in the mobile phase inside the glutted stationary phase is easier and

TABLE VII

PARAMETERS CORRESPONDING TO FIG. 2

Lines 4 and 6 correspond to static determinations.

Temperature (°C)	*Line No.*	*Slope*	*Intercept*	r^2	γ_m	$\gamma_s D_s/D_m$
25	1	0.380	2.64	0.990	1.32	0.190
	2	0.265	3.00	–	1.50	0.135
	3	0.510	2.34	–	1.17	0.255
	4	0.528	2.215	0.997	1.11	0.264
40	5	0.172	3.62	0.652	1.81	0.086
	6	0.721	1.92	0.991	0.96	0.361
22	–[a]	0.254	2.07	0.824	1.04	0.127
	–[b]	0.314	2.33	0.924	1.17	0.159

[a] 3- and 6-μm Zorbax C_8 phase.

[b] 3- and 6-μm Zorbax C_{18} phase, from Table I in ref. 24.

faster than diffusion in the bulk mobile phase. Given the porous structure of the packing material, this seems highly unlikely.

The model we used may be questioned. Crombeen *et al.*[26] showed that the additivity of diffusional fluxes, as used in eqns. 14, 21 and 22, only applied in cases where diffusion pathways in the two phases were parallel. In a random structure such as a porous particle packing material, a non-linear model must be set up[26]. In contrast, to explain the high B values that they obtained, Stout *et al.*[24] suggested again the possible importance of surface diffusion.

We think that the main reason why γ_m factors higher than unity were not previously reported is the use of the efficiency computation method. In most previous studies[3–10,22,23,26], band broadening was calculated assuming Gaussian peaks. The raw efficiency data in Table IV show that the higher the flow-rate, the greater is the overestimation of the Gaussian plate number. The overestimation was between 3% at lower flow-rates (78 μl/min) and 90% at higher values (1.25 ml/min). Reduced plate heights calculated from overestimated plate numbers are obviously lower than those which we calculated using the exact second moment method. This led to different computer fits with the Knox equation, namely lower A, B and C values. The pertinence of the use of the moment method was shown in the static method measurements: the D_{eff} coefficients, obtained using the moment method (Table III and Fig. 2), were significantly less scattered than the same coefficients obtained by Knox and Scott[10] using the Gaussian $0.6H$ method.

At 40°C, Fig. 2B shows that the B values were scattered ($r = 0.652$, Table VII). The results for benzene and toluene were poorly reproducible for unknown reasons (relative standard deviations 20, 20, 11 and 10% for benzene, toluene, ethylbenzene and propylbenzene, respectively). However, the results of the arrested elution method were less scattered and produced a significant straight line ($r = 0.991$, Table VII). This line gave an intercept allowing a γ_m factor of 0.96 to be calculated.

The $\gamma_s D_s/D_m$ values were between 0.13 and 0.27 at 25°C and 0.36 at 40°C. They can be compared with the slopes of the $(q/C)\,[(k' + \varphi)/(1 + k')]^2$ *versus* k' plots (Table VI). Both sets of data seem consistent with $q = 2/15$. The slopes obtained with $q = 1/30$ in eqn. 9 are too low. For valid C values, the γ_{sm} values were lower than unity. The $\gamma_s D_s/D_m$ values obtained using the C values in ref. 24 would be consistent with those obtained using the corresponding B values with $q = 1/15$ in eqn. 9. However, the γ_{sm} value obtained for Zorbax C_8 seems very high. Given the low accuracy of C determinations and the poor regression coefficients in Table VI, the $\gamma_s D_s/D_m$ values were not considered further.

All results of this work were obtained on the same densely grafted phase. In order to confirm these results, experiments on densely grafted octadecyl- (C_{18}), undecyl- (C_{11}) and cynodecylsilica are in progress in our laboratory.

REFERENCES

1 A. J. P. Martin and R. L. M. Synge, *Biochem. J.*, 35 (1941) 1358.
2 J. C. Giddings, *Dynamics of Chromatography*, Marcel Dekker, New York, 1965.
3 J. H. Knox and M. Saleem, *J. Chromatogr. Sci.*, 10 (1972) 80.
4 G. J. Kennedy and J. H. Knox, *J. Chromatogr. Sci.*, 10 (1972) 549.
5 J. N. Done and J. H. Knox, *J. Chromatogr. Sci.*, 10 (1972) 606.
6 J. H. Knox, *J. Chromatogr. Sci.*, 17 (1977) 352.

7 E. Grushka, L. R. Snyder and J. H. Knox, *J. Chromatogr. Sci.*, 13 (1975) 25.
8 L. R. Snyder, *J. Chromatogr. Sci.*, 7 (1969) 352.
9 J. F. K. Huber, *J. Chromatogr. Sci.*, 7 (1969) 86.
10 J. H. Knox and H. P. Scott, *J. Chromatogr.*, 282 (1983) 297.
11 A. Einstein, *Ann. Phys. (Leipzig)*, 17 (1905) 549.
12 J. F. Erard, L. Nagy and E. sz. Kováts, *Colloids Surf.*, 9 (1984) 263.
13 E. sz. Kováts, *Ger. Pat.*, 2 930 516, 1979.
14 D. Morel and J. Serpinet, *J. Chromatogr.*, 248 (1982) 231.
15 D. Morel, J. Serpinet, J. M. Letoffe and P. Claudy, *Chromatographia*, 22 (1986) 103.
16 A. Chartier, C. Gonnet, D. Morel, J. L. Rocca and J. Serpinet, *J. Chromatogr.*, 438 (1988) 263.
17 F. Gobet and E. sz. Kováts, *Adsorpt. Sci. Technol.*, 9 (1984) 77.
18 B. A. Bidlingmeyer and F. V. Warren, *Anal. Chem.*, 56 (1984) 1583A.
19 J. L. Rocca, J. W. Higgins and R. G. Brownlee, *J. Chromatogr. Sci.*, 23 (1985) 106.
20 G. I. Taylor, *Proc. R. Soc. London, Ser. A*, 223 (1954) 446.
21 R. Aris, *Proc. R. Soc. London, Ser. A*, 223 (1954) 538.
22 J. H. Knox and L. McLaren, *Anal. Chem.*, 36 (1964) 1477.
23 J. H. Knox and A. Pryde, *J. Chromatogr.*, 112 (1975) 171.
24 R. W. Stout, J. J. DeStephano and L. R. Snyder, *J. Chromatogr.*, 282 (1983) 263.
25 Cs. Horváth and H.-J. Lin, *J. Chromatogr.*, 149 (1978) 43.
26 J. P. Crombeen, H. Poppe and J. C. Kraak, *Chromatographia*, 22 (1986) 319.